Pekka Alitalo, Frédéric Bongard, Juan Mosig, and Sergei Tretyakov. 2009. Backward-wave slab with electrically tunable index of refraction. In: Proceedings of the 3rd European Conference on Antennas and Propagation (EuCAP 2009). Berlin, Germany. 23-27 March 2009, pages 1667-1671.

Backward-wave slab with electrically tunable index of refraction

Pekka Alitalo [#,*1], Frédéric Bongard [*2], Juan Mosig [*3], Sergei Tretyakov [#4]

[#]*Department of Radio Science and Engineering / SMARAD Center of Excellence, TKK Helsinki University of Technology*
Otakaari 5 A, 02150 Espoo, Finland
[1]pekka.alitalo@tkk.fi
[4]sergei.tretyakov@tkk.fi

[*]*Laboratory of Electromagnetics and Acoustics (LEMA), Ecole Polytechnique Fédérale de Lausanne (EPFL)*
Bâtiment ELB, Station 11, CH-1015 Lausanne, Switzerland
[2]frederic.bongard@epfl.ch
[3]juan.mosig@epfl.ch

***Abstract*— In this paper we demonstrate the electrical tunability of a free-space-matched backward-wave slab, composed of three-dimensionally arranged and periodically loaded transmission lines. The host transmission-line network is composed of microstrip lines, whereas the loading is achieved with lumped capacitors and inductors. As the capacitors can be easily replaced by electrically tunable varactors, we study the tunability of the slab, i.e., the tunability of the effective refractive index, and the effect of this tuning on the impedance of the slab.**

I. Introduction

Loaded transmission-line (TL) networks have been found to be a relatively easy way of implementing exotic materials, often referred to as "metamaterials" [1], [2]. The non-resonant behaviour of these networks has enabled the creation of, e.g., structures with wide-band negative index of refraction [1]–[4], and even devices that can overcome the diffraction-limit of image resolution [5], [6].

In this paper, we study the tunability of a previously presented backward-wave slab, composed of a three-dimensional, capacitively and inductively loaded transmission-line network that can be matched, e.g., to free space [7]. By replacing the lumped capacitors in the network with varactors, we can obtain a slab with electrically tunable index of refraction. The tuning naturally affects the impedance characteristics of the slab and thus the coupling with the surrounding medium. The tuning of the refractive index and its effect on the impedance are first studied analytically and the results are compared to full-wave simulations.

II. Transmission-line network

Here we use the three-dimensional host TL network introduced in [7]. The network consists of three-dimensionally arranged microstrip transmission lines. The three-dimensionality of this type of network refers to three-dimensional isotropic propagation of waves of voltages and currents inside the network. No field polarization inside this "material" can therefore be defined [8].

In [7] the host network was periodically loaded by lumped series capacitors and shunt inductors, which enabled backward-wave propagation inside the network [1], [2]. A finite-thickness slab made of this loaded network was then coupled with the surrounding free space by using a "transition layer" composed of gradually enlarging parallel-strip transmission lines [7], [9]. Negative refraction occurring at the slab interfaces, with the slab having approximately the refractive index equal to -1, was confirmed in [7] using full-wave simulations conducted with the Ansoft HFSS software.

The dispersion and impedance properties of the studied type of three-dimensional loaded TL networks were calculated by performing a periodic structure analysis on a circuital representation of the unit cell [3]. The resulting expressions were used for the design of a particular backward-wave network in [7]. The corresponding values for the circuit parameters are recalled in Table I, where d is the size of the (cubic) unit cell, Z_{TL} is the characteristic impedance of a single section of microstrip lines forming the host network, and C and L are the capacitance and inductance of the lumped loading elements.

In the full-wave simulations, the lumped capacitive and inductive loading elements are represented by surface impedance boundaries, to which we can assign the analytically calculated values [7]. The simulations however demonstrated that the desired operation of the network, with impedance matching to free space and the index of refraction approximately equal to -1 at the frequency of 4 GHz, were achieved with values of the lumped elements different from the analytically estimated optimal values shown in Table I [7]. This difference is now confirmed to be a result of the fact that the capacitance and inductance values assigned to a lumped element in the used simulation software may be different from the *effective* values of these elements, seen by the host TL network.

In order to determine the effective C and L values of

TABLE I
Analytically derived values for the network for optimal operation at 4 GHz [7]

d [mm]	Z_{TL} [Ω]	C [pF]	L [nH]
8	150	0.1	2.5

TABLE II

VALUES OF CAPACITANCE AND INDUCTANCE ASSIGNED IN THE FULL-WAVE SIMULATION MODEL [7], TOGETHER WITH THEIR EFFECTIVE VALUES

	C [pF]	L [nH]
Assigned value	0.1	2.0
Effective value	0.1185	2.588

the lumped elements with which the desired operation of the slab was achieved in [7], we have conducted simulations of single lumped L and C elements, as those used in simulations of the slab. The effective values of these elements are then extracted by fitting the resulting S-parameters to those of a two-port network composed of either a series capacitance or a shunt inductance. Using this technique, the effective values of the lumped elements that led to the desired matching and refraction properties of the slab in [7] have been extracted, showing good agreement with the analytically determined optimal values, as shown in Tables I and II.

The reason for the difference between the assigned and effective values in Table II is related to the finite sizes of the lumped elements in the simulation model. In [7] the length of the capacitive lumped elements was 0.5 mm, whereas the length of the inductive elements was 2 mm (equal to the height of the microstrip line). As shown in Table II, the effective inductance of the lumped inductors is much larger than the assigned value. This is due to the parasitic inductance of the finite-size lumped element itself. For the capacitance, the effective value is somewhat larger than the assigned value due to the parasitic capacitance of the gap in the microstrip line, where the lumped element is placed. By simulating the gap alone, it was found that this parasitic capacitance is equal to 0.0185 pF, as can also be concluded from Table II.

For analysis of the simulated model, it is important to check what are the analytically calculated refractive index and the network impedance for these effective values. For the values $C = 0.1$ pF and $L = 2.5$ nH, the effective refractive index of the backward-wave slab is equal to $n = -1$ at the frequency $f = 4.04$ GHz, while the impedance of the network equals 377 Ω at exactly 4 GHz. For the *effective* values shown in Table II, which should be used when evaluating the simulation results, these frequencies are 3.93 GHz and 3.97 GHz, respectively. By using the effective L and C values, we can now estimate the refractive index of the slab studied in [7] to be $n \approx -0.82$ at 4 GHz. These values correspond well to the previously presented results of the full-wave simulated reflection and transmission, as well as to the observed negative refraction occurring at the slab interfaces [7].

III. ELECTRICAL TUNABILITY OF THE REFRACTIVE INDEX

The main question that we want to address in this paper, is how much can we tune the refractive index of the backward-wave slab by changing the values of the lumped capacitors, and how this tuning will affect the impedance and matching characteristics of the slab. In practice, this tuning can be accomplished, e.g., by using varactors in place of the lumped capacitors.

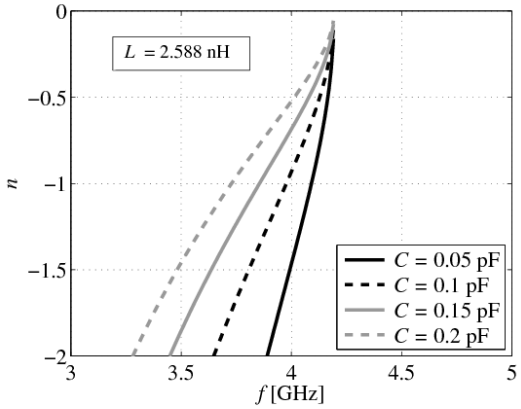

Fig. 1. Analytically calculated refractive index n of the TL network (for axial propagation), as a function of the frequency.

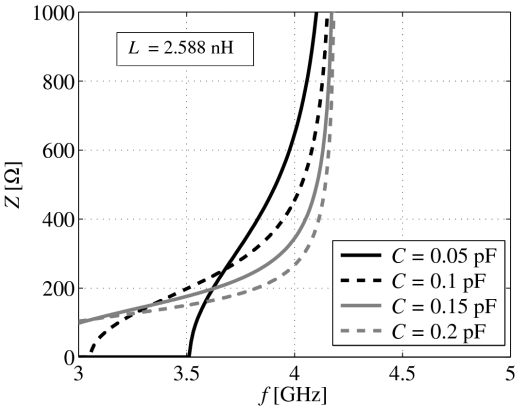

Fig. 2. Analytically calculated impedance of the TL network (for axial propagation), as a function of the frequency.

A. Dispersion and impedance

First, we will have a look at the dispersion behaviour of the network analytically, using the same methods as described in [3], [7]. By tuning the capacitance of the varactors from 0.05 pF to 0.2 pF, the refractive index n of the network is changed approximately from $n \approx -1.47$ to $n \approx -0.52$ at the frequency of 4 GHz, as shown in Fig. 1. In this calculation, the lumped shunt inductance inserted in the network is equal to $L = 2.588$ nH, as we intend to conduct the simulations of the studied slab with the previously used simulation model [7]. Although only axial propagation is considered in Fig. 1, it can be shown that propagation in the network at the frequencies of interest is effectively isotropic, as the network period (the unit cell size) is considerably smaller than the wavelength [8].

By tuning the capacitance, the impedance of the network varies as shown in Fig. 2. Although the impedance varies quite strongly as the capacitance is changed, the values of the impedance around the frequency of 4 GHz are still relatively close to the free-space wave impedance value of 377 Ω, except

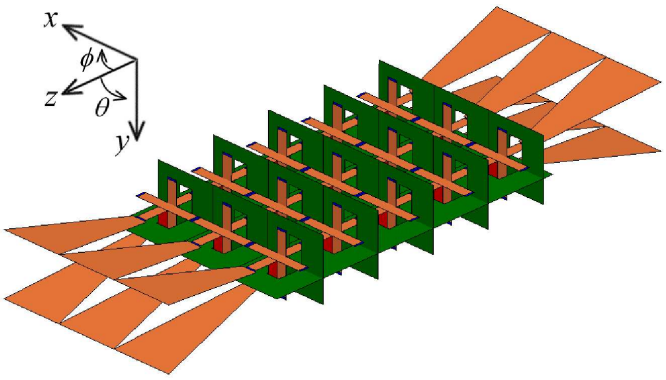

Fig. 3. HFSS model of the backward-wave slab. The metal strips of the host transmission lines and the transition layers are illustrated in orange, the ground in green, and the lumped capacitors and inductors in blue and red, respectively. The slab is periodically infinite in the x- and y-directions. On both sides of the transversally infinite slab is free space. Three unit cells are modelled along the x-direction for the visualization of wave refraction.

for the case $C = 0.05$ pF, for which the analytically calculated network impedance is as high as $Z \approx 648\ \Omega$. By tuning also the inductance L together with the capacitance C it would be possible to control also the impedance of the network along with the refractive index. This tuning of both values simultaneously is out of the scope of this paper, and would be difficult to realize in practice. Therefore, in section IIID we will study, using numerical simulations, how the tuning of the capacitance alone changes the refractive index, and more importantly, how it affects the coupling between the backward-wave slab and the surrounding free space.

B. Simulation model

The performance of the designed backward-wave slab, with the variable capacitance value, has been evaluated using the commercial full-wave simulation software Ansoft HFSS. The simulation model of the backward-wave slab is the same as studied previously [7]. The slab is modelled as effectively infinite in the transversal directions (along x and y), by assigning periodic boundaries at the top and bottom, as well as on the sides of the simulation model shown in Fig. 3.

The reflection, refraction and transmission properties of this slab can be conveniently studied by exciting the model with plane waves of different incidence angles, impinging on the slab from free space. The incident, reflected, and transmitted powers are easily calculated from the simulated fields.

C. Full-wave simulations with constant capacitance

Negative refraction with refractive index of the slab close to $n = -1$ was observed for the backward-wave slab with effective capacitance $C_{\text{eff}} = 0.1185$ pF and effective inductance $L_{\text{eff}} = 2.588$ nH (see Table II) in [7]. Here we first study the case with these capacitance and inductance values for different incidence angles in two orthogonal planes. The simulated reflection (ρ) and transmission (τ) coefficients for this slab, as functions of the incidence angles ϕ and θ are shown in Fig. 4.

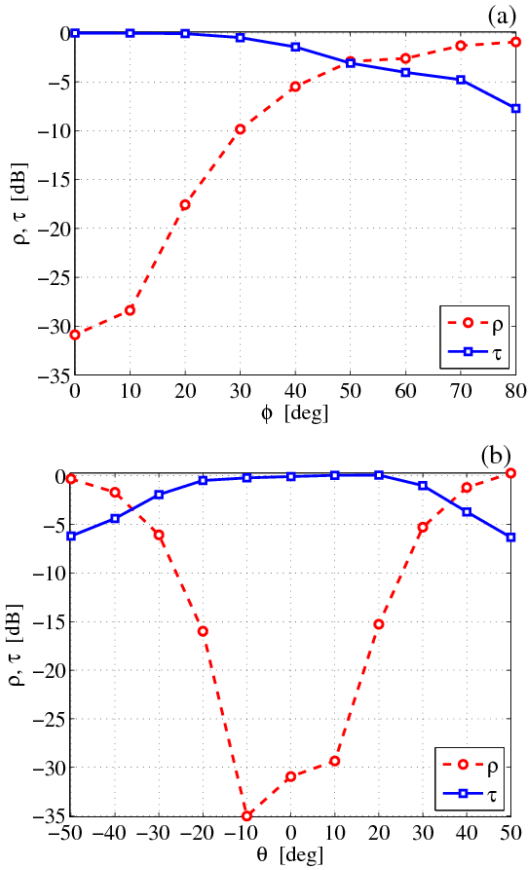

Fig. 4. Simulated reflection (red circles) and transmission (blue squares) for the backward-wave slab at the frequency 4 GHz, as a function of the incidence angles ϕ (a) and θ (b). $C_{\text{eff}} = 118.5$ fF and $L_{\text{eff}} = 2.588$ nH.

From Fig. 4a we can conclude that for the variation of the angle ϕ (the angle in the xz-plane, with the electric field $\overline{E}$ parallel to the y-axis), the coupling between the slab and free space is very good. Because the effective refractive index of the slab is not exactly equal to $n = -1$ at 4 GHz, but instead approximately $n \approx -0.82$ (see the discussion on the effective capacitance and inductance in Section II), total reflection of the wave impinging on the slab from free space should occur approximately at the angle $\phi \approx 56°$. This is in good agreement with the results in Fig. 4a.

Results for the angle θ (the angle in the yz-plane with the magnetic field $\overline{H}$ parallel to the x-axis) are shown in Fig. 4b. Here the coupling is also shown to be very good, but slightly worse than for the angle ϕ. This is of course expected since the transition layer is designed for TE-polarization, i.e., for waves with the electric field parallel to the y-axis. It must be noted that because the slab structure is symmetric with respect to the yz-plane, in Fig. 4a it is sufficient to study angles ϕ only from 0° to 90°. For the incidence angle θ, on the other hand, both negative and positive values should be studied as in Fig. 4b, although the response of ρ and τ are shown to be almost symmetric with respect to the xz-plane.

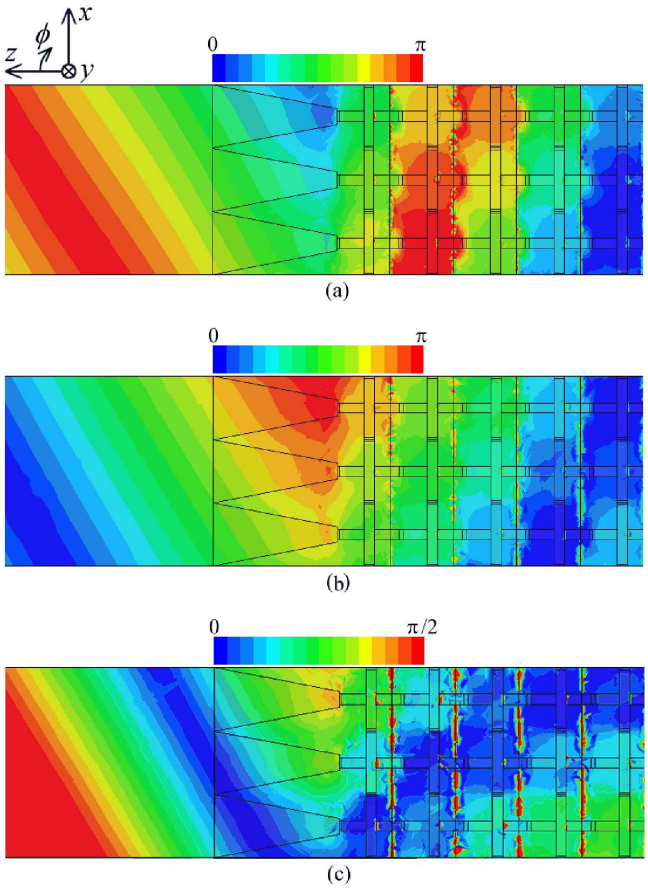

Fig. 5. Simulated phase of electric field (absolute value) around the interface between free space and the backward-wave slab at the frequency 4 GHz. Free space on the left and the backward-wave slab on the right. The incidence angle of the plane wave impinging on the slab (from the right side) is $\phi = 30°$. (a) $C_{\text{eff}} = 44$ fF and refractive index of the slab $n \approx -1.6$. (b) $C_{\text{eff}} = 94$ fF and refractive index of the slab $n \approx -1.0$. (c) $C_{\text{eff}} = 144$ fF and refractive index of the slab $n \approx -0.7$.

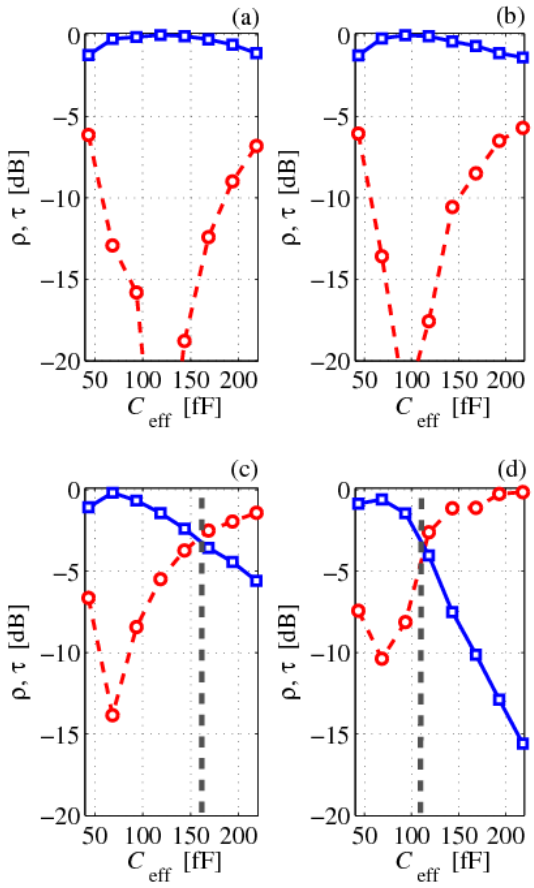

Fig. 6. Simulated reflection (red circles) and transmission (blue squares) for the backward-wave slab at the frequency 4 GHz, as a function of the *effective* capacitance of the loading varactors. (a) $\phi = 0°$. (b) $\phi = 20°$. (c) $\phi = 40°$. (d) $\phi = 60°$. The grey dashed lines in (c) and (d) illustrate the analytically estimated point of total reflection.

D. Full-wave simulations with variable capacitance

Instead of having a constant capacitance, here the effective capacitance of the lumped capacitors is varied from approximately 0.04 pF to 0.22 pF, while having constant $L_{\text{eff}} = 2.588$ nH. For simplicity, in the following we will study the tunability of the slab only for incidence angles in the xz-plane (TE-polarization), i.e., for different angles of ϕ. First we check that the change in the refractive index due to the change in C_{eff} is visible in the simulated fields. This can be done by illuminating the studied backward-wave slab with a plane wave having a certain angle of incidence, and then studying the simulated field distributions. These results for the incidence angle $\phi = 30°$ are presented in Fig. 5, where the electric field phase is plotted for three different values of C_{eff}. The studied values of the capacitance C_{eff} are 44 fF, 94 fF and 144 fF, corresponding to the analytically calculated refractive indices of $n \approx -1.6$, $n \approx -1.0$ and $n \approx -0.7$, respectively.

The change in the refractive index of the simulated slab can be clearly seen. In Fig. 5a the refraction angle is small and the wavefront inside the slab clearly propagates close to the normal direction because $|n| > 1$. For the case in Fig. 5b, the refractive index is -1 and the angle of negative refraction is approximately equal to the incidence angle. In Fig. 5c, on the other hand, the refraction angle is large, because $|n| < 1$. In Fig. 5c the absolute value of the phase is plotted only up to $\pi/2$ to have a more illustrative picture of the refraction phenomenon (the wavelength is increased as compared to Figs. 5a and 5b).

To study the coupling between the slab and the surrounding free space, we have simulated plane-wave reflection and transmission through the slab, varying the incidence angle and the value of the effective capacitance. The results for reflectance and transmittance as functions of C_{eff} are shown for angles $\phi = 0°$, $\phi = 20°$, $\phi = 40°$ and $\phi = 60°$ in Fig. 6. The transmission through the slab is relatively high ($\tau > -3$ dB) for all angles and all studied values of C_{eff}, in the regions where total reflection does not occur.

For the cases $\phi = 0°$ and $\phi = 20°$, total reflection does not happen at any values of C_{eff}, but for the cases $\phi = 40°$ and $\phi = 60°$, total reflection occurs when $n >$

-0.64 (corresponding to $C_{\rm eff} > 169$ fF) and $n > -0.86$ (corresponding to $C_{\rm eff} > 111$ fF), respectively. These values of $C_{\rm eff}$ are marked in Figs. 6c and 6d and in both cases this point is very close to the -3 dB levels in both transmittance and reflectance. Thus, the studied backward-wave slab is shown to be well coupled to the surrounding free space for a wide range of incidence angles and values of $C_{\rm eff}$, for which total reflection due to the effective refractive index does not occur.

IV. Conclusions

The electrical tunability of a three-dimensional periodically loaded transmission-line network has been investigated. The network is loaded with lumped series capacitors and shunt inductors, thus enabling backward-wave propagation in the structure. The coupling of a slab composed of this network with free space is realized with a transition layer composed of gradually enlarging parallel-strip transmission lines. The effect of the tuning of the lumped capacitances, which can in practice be realized with varactors, is studied analytically and with numerical simulations. This tuning is shown to be able to change the effective refractive index of the slab at a fixed frequency, while good coupling between the backward-wave slab and the surrounding free space is maintained.

Acknowledgment

This work has been partially supported by TEKES through the Center-of-Excellence program. P. Alitalo wishes to thank Mr. O. Luukkonen for discussions and help with the simulations. During this work P. Alitalo was an invited researcher at EPFL-Switzerland. P. Alitalo acknowledges financial support by GETA, the Emil Aaltonen Foundation, and the Nokia Foundation.

References

[1] G. V. Eleftheriades and K. G. Balmain, Eds., *Negative-Refraction Metamaterials: Fundamental Principles and Applications*. Hoboken, NJ: John Wiley & Sons, 2005.

[2] C. Caloz and T. Itoh, *Electromagnetic Metamaterials: Transmission Line Theory and Microwave Applications*. Hoboken, NJ: John Wiley & Sons, 2006.

[3] P. Alitalo, S. Maslovski, and S. Tretyakov, "Three-dimensional isotropic perfect lens based on lc-loaded transmission lines," *J. Appl. Phys.*, vol. 99, p. 064912, 2006.

[4] ——, "Experimental verification of the key properties of a three-dimensional isotropic transmission-line superlens," *J. Appl. Phys.*, vol. 99, p. 124910, 2006.

[5] A. Grbic and G. V. Eleftheriades, "Overcoming the diffraction limit with a planar left-handed transmission-line lens," *Phys. Rev. Lett.*, vol. 92, p. 117403, 2004.

[6] A. K. Iyer and G. V. Eleftheriades, "Mechanisms of subdiffraction free-space imaging using a transmission-line metamaterial superlens: An experimental verification," *Appl. Phys. Lett.*, vol. 92, p. 131105, 2008.

[7] P. Alitalo, O. Luukkonen, and S. Tretyakov, "A three-dimensional backward-wave network matched with free space," *Phys. Lett. A*, vol. 372, pp. 2720–2723, 2008.

[8] P. Alitalo and S. Tretyakov, "Sub-wavelength resolution with three-dimensional isotropic transmission-line lenses," *Metamaterials*, vol. 1, no. 2, pp. 81–88, 2007.

[9] P. Alitalo, O. Luukkonen, L. Jylha, J. Venermo, and S. A. Tretyakov, "Transmission-line networks cloaking objects from electromagnetic fields," *IEEE Transactions on Antennas and Propagation*, vol. 56, pp. 416–424, 2008.